

Evolution of a nanoflare-scale magnetic reconnection event in the quiet Sun

Rebecca A. Robinson 

Rosseland Centre for Solar Physics, University of Oslo, PO Box 1029, Blindern 0315, Oslo, Norway

email: becca.anne.robinson@gmail.com

Abstract. Low-lying loops in the quiet Sun are a reliable source of energy for atmospheric heating, but the mechanisms by which they evolve are somewhat enigmatic. To address the origins of atmospheric heating events in the quiet Sun, we utilize our stratified, convection-driven, 3D MHD simulation Bifrost to explore the evolution and eventual major reconnection between several magnetic features; one of which is a magnetic flux rope. We zoom in on the buildup of the magnetic flux rope, which self-orders in the corona via an inverse cascade of helicity. We also discover that the flux rope attempts to relax to a linear force-free field according to Taylor's theory, but cannot do so completely. Finally, we demonstrate that the eventual nanoflare-scale reconnection event could potentially be observed in the 171 Å channels of SDO/AIA and the future MUSE mission. We also determine that the spectral resolution of MUSE is sensitive enough to capture the kinematics of the bi-directional plasma jets emanating from the reconnection region.

Keywords. Sun: magnetic fields, Sun: activity, Sun: atmosphere, Sun: corona, Sun: flares

1. Introduction

Nanoflares are small, bright events on the Sun that are associated with localized atmospheric heating in the solar corona. Their potentially ubiquitous distribution makes them good candidates for sustained coronal heating, but their size makes it challenging to observe and understand them. With that, a combination of theory, observations, and simulations can help inform and expand our understanding of how these events occur. We present a simulation of a nanoflare-scale event that is powered by the large-angle reconnection of a magnetic flux rope and magnetic arcade with an overlying, nearly antiparallel horizontal field in the corona.

2. Methods

2.1. *The Bifrost simulation*

The simulation presented here is a quiet Sun simulation produced with the Bifrost code (Gudiksen et al. 2011), a massively parallel MHD code that simulates stellar atmospheres from the convection zone to the corona. The specifics of the simulation are described in detail in Robinson et al. (2022), Robinson et al. (2023), and Robinson and Carlsson (2023), but I will briefly summarize the important characteristics here.

Our simulation domain is a small cube of solar atmosphere with a 12 Mm horizontal extent in each horizontal direction, and a vertical extent from 2.5 Mm below the average solar surface ($z = 0$) to 8 Mm above it. The horizontal resolution is a uniform 23 km, whereas the vertical resolution is variable and sharpest between $z = 2$ and $z = 4$ Mm. The convective boundary allows inflows as long as the effective temperature is consistent

with the temperature of photospheric plasma, and the coronal boundary is open. The horizontal boundaries are periodic, meaning that features can exit and reenter the box as physically required. This allows magnetic field lines (for example) to cross the horizontal boundaries but still find magnetic roots in the photosphere, which encourages the buildup of magnetic twist.

The initial magnetic field is a free parameter in Bifrost, and the main phase of this run began with an initially balanced vertical field extrapolated to a potential field. Then, convective drivers process this initially balanced field to evolve it further. Interactions between the magnetic field lines are mitigated by our hyper-diffusion parameters, which prevent diffusive regions from breaching the numerical resolution (see Færder et al. 2023). With these parameters, the energy from magnetic reconnection is still conserved but deposited in a more diffusive manner; this effect is similar to dramatically increasing the resolution of the simulation in diffusive regions.

Bifrost comes with an optional module called `corks`, described in detail in Robinson et al. (2022), Robinson et al. (2023), and Robinson and Carlsson (2023). This module introduces non-interacting test particles into the simulation, which are advected with the ideal flow of the fluid. We also assume that the magnetic field lines follow ideal transport outside of diffusive regions, which means that individual corks can trace individual magnetic field lines. This method of using corks to follow particular magnetic features was used throughout the presented study.

2.2. Calculating synthetic observables

To determine whether the nanoflare-scale event could be observed by modern and future instruments, we calculated the synthetic intensities of two iron ions that form under optically thin conditions in the solar corona. The CHIANTI database (Del Zanna et al. 2021) was used to calculate synthetic spectra of Fe IX at 171 Å and Fe XII at 195 Å, integrating both along the z axis as well as the y axis. This provided a top-down and a side view of the nanoflare-scale event, which provided two viewing angles for analysis. The first moments of the spectra were also calculated in order to understand the Doppler signatures of the event.

3. Results

3.1. Finding relevant magnetic features

The simulation described in Section 2.1 resulted in impulsive heating events that produced local coronal plasma temperatures up to 1.47 MK. The cause of the heating was found to be large-angle reconnection between several magnetic features as shown in Fig. 1, which were identified using the aforementioned `corks` module. Corks were selected based on their proximity to current volumes that formed as a result of large-angle reconnection. Then, the same corks were used to reconstruct a time series of the relevant features.

We determined that the magnetic features did not rise coherently through the atmosphere, but rather self-order in the corona throughout the duration of the simulation (Robinson et al. 2022). Additionally, no relevant flux cancellation events are observed; the photospheric flux concentrations to which the magnetic features are rooted remain steadfast during the time leading up to the reconnection. Therefore, the reconnection event is not associated with traditional magnetoconvective processes such as flux emergence or flux cancellation.

3.2. Buildup of the flux rope

Because the nanoflare-scale reconnection event is powered by the gradual buildup of a magnetic flux rope, we set out to understand how the flux rope self-consistently forms.

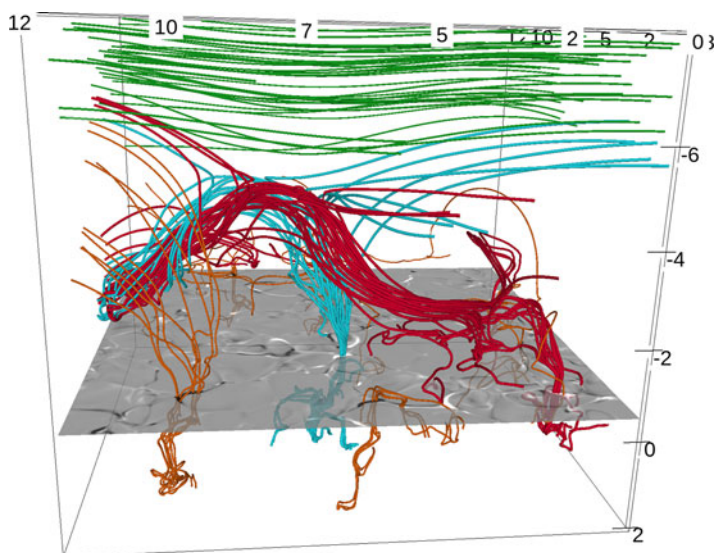


Figure 1. Visualization of relevant magnetic features at $t = 11360$ s. Cyan lines represent a magnetic arcade, and red lines represent a magnetic flux rope. The overlying horizontal field (green) is nearly anti-parallel to the red and cyan features.

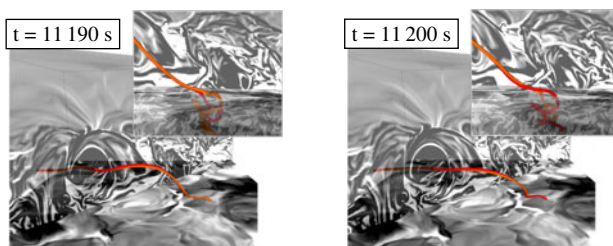


Figure 2. Field line pair at $t = 11190$ s (left) and $t = 11200$ s (right) that are traced by the same two corks, but switch chromospheric footpoints between the time stamps. The insets in the upper right corners offer a zoomed-in view of the footpoint switching at a different viewing angle, as evidenced by the lines switching colors.

To do this, we searched for evidence of the inverse cascade of helicity (Frisch et al. 1975; Pouquet et al. 2019), whereby the self-helicities of smaller flux bundles coalesce by reconnection, and contribute to a larger-scale helical system. To that end, we detected such a helicity cascade evidenced by not only small-scale flux bundles but by individual magnetic field line pairs undergoing component reconnection. This component reconnection was detected by isolating individual field pairs that belong to the overall flux rope, and that switch footpoints over a chromospheric slice as shown in Fig. 2. From this, we determine that the self-helicities of these magnetic field line pairs contribute to the helicities of small-scale flux bundles via component reconnection, which themselves coalesce to form the overall flux rope.

In addition to this, the flux rope tends toward a linear force-free field after it forms (that is, undergoes Taylor relaxation, see Taylor (1974)). In a constantly driven system that eventually undergoes major reconnection, the flux rope is of course unable to fully relax according to Taylor's theory; however, we see a statistical tendency toward Taylor relaxation during the time the flux rope is forming via the inverse cascade of helicity

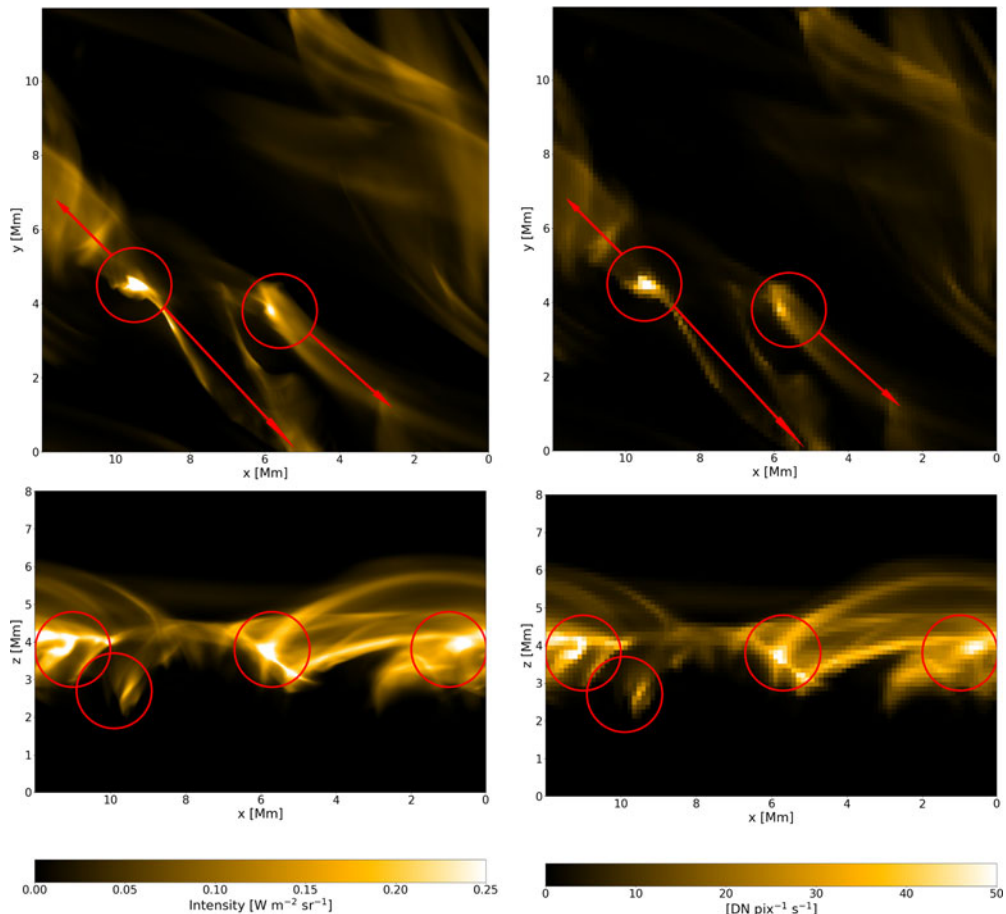


Figure 3. Synthetic intensities at the native simulation resolution for Fe IX 171 Å (left) compared to synthetic MUSE intensities (right) at $t = 11\,360$ s. Bright points of interest are denoted with red circles, and the two jet systems in the upper panels are denoted with red arrows. Synthetic MUSE observations are degraded to the highest possible resolution of $0.167''$.

(Robinson et al. 2023). This is a result that had not been produced in idealized simulations because Taylor relaxation requires a significant number of reconnections and that is only possible for a more complex simulation.

3.3. Synthetic observables

Our final result concerns the observability of the nanoflare-scale event previously discussed. As mentioned in Section 2.2, we consider the signatures of both Fe IX and Fe XII at a reference snapshot during the nanoflare-scale event, converting their integrated intensities from physical units to telescope count rates for the Solar Dynamics Observatory Atmospheric Imaging Assembly (SDO/AIA; Pesnell, Thompson, and Chamberlin 2012; Lemen et al. 2012) and the Multi-slit Solar Explorer (MUSE; De Pontieu et al. 2020, 2022; Cheung et al. 2022). We determine that the count rates would be sufficient for observation in the Fe IX 171 channel for both SDO/AIA and MUSE (Robinson and Carlsson 2023). In particular, two systems of bi-directional jets emanating from the reconnection spine would be observable with both instruments, as shown for MUSE in Fig. 3. However, the integrated intensities for Fe XII at 195 Å would not be visible in the SDO/AIA 193

channel because calculated count rates are insufficient. We note that MUSE will not be designed to observe Fe XII, but the spectral resolution of MUSE is sufficient for detecting the Doppler shifts of the bi-directional jets. This serves as a support for MUSE and also contextualizes past and future observations of nanoflare-scale reconnection events that are not associated with flux emergence or flux cancellation.

4. Discussion

The described studies provide insight into the development of magnetic fields that contribute to energetic nanoflare-scale reconnection events in the quiet Sun. Not only did we simulate such an event in a self-consistent manner, but we determined that the event forms from coronal magnetic field lines rather than by more traditional magnetoconvective processes. We also demonstrate how this event would appear in observations of Fe IX 171Å, and look forward to the new capabilities of the upcoming MUSE instrument.

4.1. Scientific discussion at the symposium

During the symposium, the discussion focused mostly on the inverse cascade of helicity. First, it was suggested that the small-scale component reconnections may be evidence of the interchange instability. This is an interesting suggestion, but we do see evidence of topological changes rather than an interchange between the field and the surrounding plasma.

There was also a brief discussion regarding why the helicity cascade is inverse rather than forward. We of course still see a forward cascade of energy, so why not a forward cascade of helicity? In this case, we neither see nor consider any larger-scale helical systems that may disintegrate into small-scale helical systems; instead, we observe small-scale helical systems contributing to an overall large-scale system. This inverse helicity cascade is most relevant for the nanoflare-scale reconnection event because the development of the flux rope via several small-scale reconnections ultimately powers the large-scale reconnection.

Acknowledgements. Figures are adapted from Robinson et al. (2022), Robinson et al. (2023), and Robinson and Carlsson (2023). RR acknowledges funding support under ERC Synergy grant agreement No. 810218 (Whole Sun).

References

- Cheung, M.C.M., Martínez-Sykora, J., Testa, P., De Pontieu, B., Chintzoglou, G., Rempel, M., and, ...: 2022, *The Astrophysical Journal* **926**, 53. doi:10.3847/1538-4357/ac4223.
- De Pontieu, B., Martínez-Sykora, J., Testa, P., Winebarger, A.R., Daw, A., Hansteen, V., and, ...: 2020, *The Astrophysical Journal* **888**, 3. doi:10.3847/1538-4357/ab5b03.
- De Pontieu, B., Testa, P., Martínez-Sykora, J., Antolin, P., Karmampelas, K., Hansteen, V., and, ...: 2022, *The Astrophysical Journal* **926**, 52. doi:10.3847/1538-4357/ac4222.
- Del Zanna, G., Dere, K.P., Young, P.R., and Landi, E.: 2021, *The Astrophysical Journal* **909**, 38. doi:10.3847/1538-4357/abd8ce.
- Frisch, U., Pouquet, A., Leorat, J., and Mazure, A.: 1975, *Journal of Fluid Mechanics* **68**, 769. doi:10.1017/S002211207500122X.
- Færder, Ø.H., Nóbrega-Siverio, D., and Carlsson, M.: 2023, *Astronomy and Astrophysics* **675**, A97. doi:10.1051/0004-6361/202346447.
- Gudiksen, B.V., Carlsson, M., Hansteen, V.H., Hayek, W., Leenaarts, J., and Martínez-Sykora, J.: 2011, *Astronomy and Astrophysics* **531**, A154. doi:10.1051/0004-6361/201116520.
- Lemen, J.R., Title, A.M., Akin, D.J., Boerner, P.F., Chou, C., Drake, J.F., and, ...: 2012, *Solar Physics* **275**, 17. doi:10.1007/s11207-011-9776-8.
- Pesnell, W.D., Thompson, B.J., and Chamberlin, P.C.: 2012, *Solar Physics* **275**, 3. doi:10.1007/s11207-011-9841-3.

- Pouquet, A., Rosenberg, D., Stawarz, J.E., and Marino, R.: 2019, *Earth and Space Science* **6**, 351. doi:10.1029/2018EA000432.
- Robinson, R.A., Carlsson, M., and Aulanier, G.: 2022, *Astronomy and Astrophysics* **668**, A177. doi:10.1051/0004-6361/202244750.
- Robinson, R.A., Aulanier, G., and Carlsson, M.: 2023, *Astronomy and Astrophysics* **673**, A79. doi:10.1051/0004-6361/202346065.
- Robinson, R.A. and Carlsson, M.: 2023, *Astronomy and Astrophysics* **677**, A36. doi:10.1051/0004-6361/202347089.
- Taylor, J.B.: 1974, *Physical Review Letters* **33**, 1139. doi:10.1103/PhysRevLett.33.1139.